

**CRYSTALLIZATION OF FERROMAGNESIAN AMORPHOUS SILICATE NANOPARTICLES WITH OLIVINE-LIKE STOICHIOMETRY SYNTHESIZED WITH THERMAL PLASMA METHOD.** R. Sakurai<sup>1</sup>, K. Kobayashi<sup>2</sup>, D. Yamamoto<sup>3</sup> and S. Tachibana<sup>3,4</sup>. <sup>1</sup>Department of Earth and Planetary Science, University of Tokyo, Tokyo 113-0033, Japan (sakurai@eps.s.u-tokyo.ac.jp); <sup>2</sup>Department of Natural History Sciences, Hokkaido University, Sapporo 060-0810, Japan; <sup>3</sup>Department of Solar System Sciences, Institute of Space and Astronautical Science (ISAS), JAXA, Sagami-hara 252-5210, Japan; <sup>4</sup>UTokyo Organization for Planetary and Space Science (UTOPS), University of Tokyo, Tokyo 113-0033, Japan.

**Introduction:** Submicron-sized amorphous silicate dust has been considered to be the main precursors of solid components in protoplanetary disks [e.g. 1, 2]. Astronomical observations indicate that amorphous silicate dust crystallizes in the protoplanetary disks due to sub-solidus thermal annealing [e.g., 2, 3]. Ferromagnesian amorphous silicate is found as the main constituent of the matrices of pristine chondritic meteorites [e.g., 4] and as presolar silicate grains [e.g., 5]. This suggests that (at least some) ferromagnesian amorphous silicate dust avoided being crystallized by thermal annealing in the Sun's protoplanetary disk.

Crystallization kinetics of amorphous silicate dust is essential for constraining the disk thermal condition to preserve amorphous silicate dust. Crystallization kinetics and mechanism of amorphous Mg silicates have been investigated and clarified in detail [6, 7], but those of ferromagnesian amorphous silicates have not yet been fully investigated. Here we synthesized ferromagnesian amorphous silicate nanoparticles with olivine ((Mg, Fe)<sub>2</sub>SiO<sub>4</sub>)-like stoichiometry with the thermal plasma method and performed crystallization experiments in vacuum to study their crystallization behavior.

**Synthesis of Amorphous Nanoparticles:** Ferromagnesian amorphous silicate nanoparticles with olivine-like stoichiometry (amorphous olivine) were synthesized by a radio-frequency inductive thermal plasma method (RF-ITP) [9] at Nisshin Engineering Inc. An ethanol-based slurry containing Fe<sub>2</sub>O<sub>3</sub>, Mg(OH)<sub>2</sub> and SiO<sub>2</sub> with the molar (Mg+Fe)/Si ratio of 2 and Fo# (Mg/(Mg+Fe) at.%) of 50 was sprayed into the 10<sup>4</sup> K plasma of Ar and O<sub>2</sub>. The source material, evaporated for ~10<sup>-2</sup> s in the plasma, was rapidly cooled with the cooling rate of 10<sup>5</sup>-10<sup>7</sup> K s<sup>-1</sup> to form nanoparticles. The redox condition in the plasma torch was changed by H/O ratio in the source materials and plasma gas. Two experimental charges were synthesized under two different H/O ratios (H/O~1.39 for the sample #10-3 and H/O~1.53 for the sample #11-1). Morphology, chemical compositions, and crystallinity of the synthesized particles were examined using field-emission scanning electron microscopy with energy dispersive X-ray spectroscopy (FE-SEM-EDS; JEOL JSM-7000F), Fourier transform infrared spectroscopy (FT-IR; JASCO

FT/IR-4200), and X-ray diffraction (XRD; PANalytical X'Pert Pro MPD) at University of Tokyo. The synthesized powder was pelletized for elemental mapping with FE-SEM-EDS.

**Crystallization Experiments in vacuum:** The #11-1 powder was used as the starting material in this study. About 30 mg of the powder was heated in a vacuum furnace at ~1×10<sup>-4</sup> Pa and 580–750°C for 1–96 hours. The experimental procedure is basically the same as [7]. The crystallization kinetics of amorphous silicate with forsterite composition (Mg<sub>2</sub>SiO<sub>4</sub>) depends on the partial pressure of H<sub>2</sub>O [7], but the present experiments were done in vacuum (~1×10<sup>-4</sup> Pa, roughly equal to the partial pressure of H<sub>2</sub>O) for simplicity.

Morphology, chemical compositions, and crystallinity of the annealed samples were examined with FE-SEM-EDS, FT-IR, and XRD (Rigaku RINT-2100).

**Results and Discussion:** The average grain size of amorphous olivine particles was ~70 nm in diameter by FE-SEM observation and the Brunauer-Emmett-Teller (BET) absorption method.

EDS analysis of the pelletized amorphous olivine powder showed that the powder has an olivine-like composition with Fo# of ~70 with patchy regions (10–20 %) with a pyroxene ((Mg, Fe)SiO<sub>3</sub>)-like composition. This could be due to contamination of pyroxene-like amorphous silicate powder synthesized prior to the amorphous olivine powder.

X-ray diffraction (XRD) patterns of #10-3 and #11-1 show broad halos at 2θ~32° that is characteristic of amorphous silicate. The #11-1 powder contain Fe-dominated phase(s) (α-iron and/or Fe<sub>3</sub>C) and approximately 1 % of crystalline olivine with Fo# of ~59, whereas the #10-3 powder contain a small amount of magnetite (Fig. 1). The presence of Fe<sup>0</sup> and ferrous Fe in #11-1 and both ferrous and ferric iron in #10-3 suggests that there may be the H/C condition that stabilize only ferrous iron between H/C of 1.39 and 1.53 in the present synthesis condition.

The infrared absorption spectrum of #11-1 shows two broad features centered at ~10 μm and 18 μm, which are attributed to the Si-O stretching and O-Si-O bending vibration modes of amorphous silicates [2], respectively (0-hour samples in Fig. 2). The spectral

shape resembles that of amorphous forsterite heated at 680°C for 3 h [5].

The samples heated in vacuum show the XRD pattern with peaks of crystalline olivine with Fo# of 53–60 that is estimated from the (130) spacing. Their infrared absorption spectra also change with time from amorphous absorption features to those of crystalline olivine. Above 680°C, sharp features at 10.2  $\mu\text{m}$  and 11.2  $\mu\text{m}$  and broad features at  $\sim 17 \mu\text{m}$  and  $\sim 19 \mu\text{m}$  appeared after 1-hour heating and remain unchanged with further heating. These peaks are attributed to crystalline olivine. At 630°C, the infrared features of olivine became prominent during the first 6-hour heating, and showed no further change after 6 h. At 580°C, the crystalline features were obscure for the first 2 hours heating but gradually appeared after 6-h heating. These temporal changes of infrared spectra suggest the faster crystallization of amorphous olivine (#11-1) than amorphous forsterite [7], which is consistent with [8, 9]. The 2-% crystallization of amorphous forsterite occurs with 18 and 231-hour heating at 630 and 580°C, respectively [7], whereas #11-1 showed obvious crystalline infrared signatures even after 0.5 and 6-h heating at 630 and 580°C (Fig. 3). Further investigation is required to obtain the crystallization kinetics and to understand the crystallization mechanism, but the observed difference in crystallization could be due to chemical and/or structural effects of ferrous iron in amorphous silicates (e.g., changes in viscosity, glass transition temperature and so on). Alternatively, this could be due to the presence of a small amount of crystalline olivine and Fe-dominated phase(s) in #11-1 that may promote heterogeneous nucleation of crystalline olivine, but amorphous forsterite used in [7] also contained a small amount of crystalline forsterite seeds.

If ferromagnesian amorphous silicates crystallize more effectively with thermal annealing than amorphous Mg silicates, the disk temperature to prevent crystallization of amorphous dust would be lower than that for amorphous Mg silicates. Moreover, the temperature range required for oxygen isotope exchange of amorphous dust with disk gas without crystallization could be narrower than that for amorphous Mg silicate dust [10, 11].

**References:** [1] Kemper F. et al. (2004) *ApJ* 609, 826–837. [2] Henning T. (2010) *Annu. Rev. A&A* 48, 21–46 [3] Molster F. J. et al. (1999) *Nature* 401, 563–565. [4] Brearley A. (1993) *GCA* 57, 1521–1550. [5] Floss C. and Haenecour P. (2016) *Geochem. J.* 50, 3–25. [6] Murata K. et al. (2009) *ApJ* 697, 836–842. [7] Yamamoto D. and Tachibana S. (2018) *ACS Earth Space Chem.* 2, 778–786. [8] Brucato J. R. et al. (2002) *Planet. Space Sci.* 50, 829–837 [9] Murata K. et al. (2007) *ApJ* 668, 285–293. [10] Yamamoto D. et al.

(2018) *ApJ* 865, 98 (14 pp). [11] Yamamoto D. et al. (2019) *MaPS*, doi.org/10.1111/maps.13365.

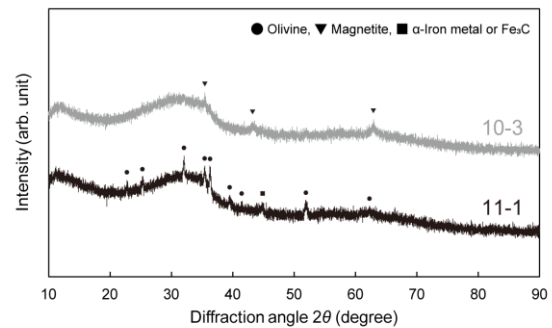


**Fig. 1.** XRD patterns of the synthesized powders of #10-3 and #11-1.

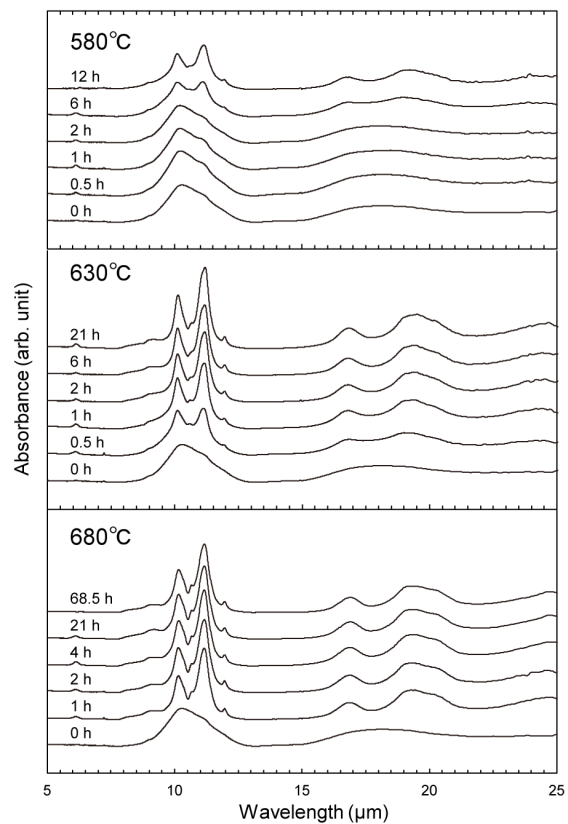


**Fig. 2.** Infrared absorption spectra of the starting material (#11-1) and run products heated at 580, 630 and 680°C in vacuum for different durations. The spectra of the run products are arbitrary shifted in the vertical direction.